Geochemistry Geophysics Geosystems G3

Article
Volume 14, Number 12
20 December 2013
doi: 10.1002/2013GC004942
ISSN: 1525-2027

Published by AGU and the Geochemical Society

Two views of Hawaiian plume structure

Albrecht W. Hofmann
Lamont-Doherty Earth Observatory of Columbia University, Palisades, New York 10964, USA

Max-Planck-Institute for Chemistry, Hahn-Meitner-Weg 1, 55128 Mainz, Germany (albrecht.hofmann@mpic.de)

Cinzia G. Farnetani
Institut de Physique du Globe de Paris, Sorbonne Paris Cité, Université Paris Diderot, UMR 7154, Paris, France

[1] Fundamentally contradictory interpretations of the isotopic compositions of Hawaiian basalts persist, even among authors who agree that the Hawaiian hotspot is caused by a deep-mantle plume. One view holds that the regional isotopic pattern of the volcanoes reflects large-scale heterogeneities in the basal thermal boundary layer of the mantle. These are drawn into the rising plume conduit, where they are vertically stretched and ultimately sampled by volcanoes. The alternative view is that the plume resembles a "uniformly heterogeneous plum pudding," with fertile plums of pyroxenite and/or enriched peridotite scattered in a matrix of more refractory peridotite. In a rising plume, the plums melt before the matrix, and the final melt composition is controlled significantly by the bulk melt fraction. Here we show that the uniformly heterogeneous plum pudding model is inconsistent with several geochemical observations: (1) the relative melt fractions inferred from La/Yb ratios in shield-stage basalts of the two parallel (Kea- and Loa-) volcanic chains, (2) the systematic Pb-isotopic differences between the chains, and the absence of such differences between shield and postshield phases, (3) the systematic shift to uniformly depleted Nd-isotopic compositions during rejuvenated volcanism. We extend our previous numerical simulation to the low melt production rates calculated far downstream (200–400 km) from shield volcanism. Part of these melts, feeding rejuvenated volcanism, are formed at pressures of ~5 GPa in the previously unmelted underside of the plume, from material that originally constituted the uppermost part of the thermal boundary layer at the base of the mantle.

Components: 11,767 words, 8 figures.

Keywords: Hawaii; isotopes; mantle plume; mantle heterogeneities.

Index Terms: 1009 Geochemical modeling: Geochemistry; 1038 Mantle processes: Geochemistry; 3610 Geochemical modeling: Mineralogy and Petrology; 3621 Mantle processes: Mineralogy and Petrology; 8410 Geochemical modeling: Volcanology.

Received 12 July 2013; **Revised** 8 November 2013; **Accepted** 15 November 2013; **Published** 20 December 2013.

Hofmann, A. W., and C. G. Farnetani (2013), Two views of Hawaiian plume structure, *Geochem. Geophys. Geosyst.*, *14*, 5308–5322, doi:10.1002/2013GC004942.

1. Introduction

[2] One of the most important aims of isotopic studies of oceanic basalts from Hawaii (and other hotspot locations) is to determine the structure and origin of the underlying mantle source. Although there is a growing (though not universal) consensus that Hawaii and at least several other major

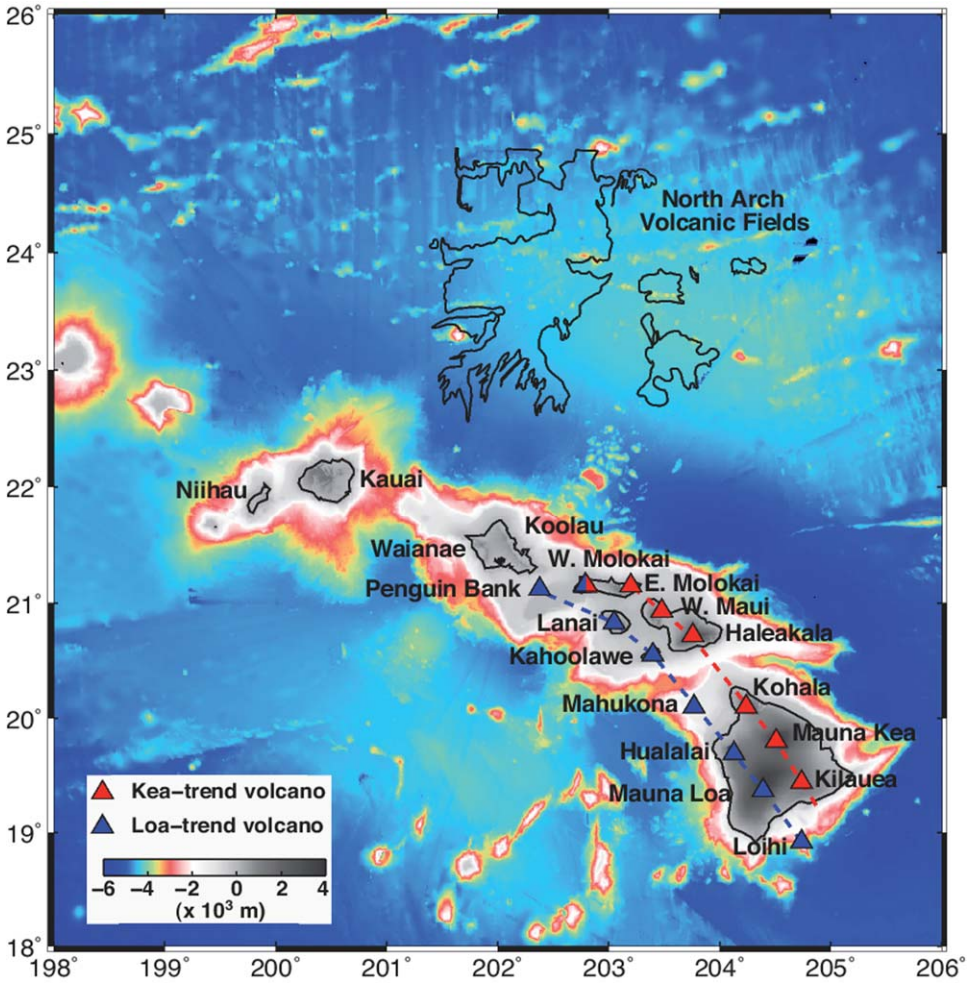

Figure 1. Location map of Hawaiian volcanoes belonging to the Loa-trend (blue triangles) and Kea-trend (red triangles), and of North Arch Volcanic Fields. West Molokai (half-red, half-blue triangle) is located between the two geographic trends. Bathymetry extracted from the GEBCO Digital Atlas published by the British Oceanographic Data Centre (https://www.bodc.ac.uk).

hotspots are generated by mantle plumes [e.g., *Kerr*, 2013], and even though most of the geochemical community subscribes to this view, there is persistent controversy about some very fundamental aspects of how to interpret the isotope data. A central question is how the isotopic signals carried to the surface by basaltic magmas should be mapped back into the melting region, in order to infer the isotopic structure of the plume. Only by knowing approximate answers to this question can we ask further how this isotopic structure can be translated back into the large-scale geochemical heterogeneities of the source region at the base of the mantle.

[3] The simplest approach, adopted by most geochemists, has been to assume that the isotopic composition of an oceanic volcano is roughly representative of its bulk source region [e.g., *Hofmann and Hart*, 1978], as exemplified by a 25–30 km radius magma capture zone beneath an Hawaiian volcano [*DePaolo et al*., 2001]. This affords the opportunity to map the internal isotopic structure of the plume, when two or more parallel loci of volcanism sample the plume "head" and when a given volcano is carried across the plume by a moving lithosphere (see Figure 1 for a map of the two Hawaiian volcanic tracks). An important question raised in this context was whether the Hawaiian plume is concentrically or bilaterally zoned [e.g., *Hauri et al*., 1996; *Kurz et al*., 1996; *Bryce et al*., 2005; *Abouchami et al*., 2005]. The interpretation of bilateral zoning, introduced by *Abouchami et al*. [2005] on the basis of a sharp distinction in both Pb and Nd isotopes between

Loa and Kea-trend volcanoes, was strongly reinforced by *Hanano et al*. [2010] who showed that the isotopic distinction between the two parallel volcanic chains extends to their respective postshield eruptive phases (though not to their rejuvenated phases; see section 5).

[4] Laboratory models by *Kerr and Mériaux* [2004] and numerical simulations by *Farnetani and Hofmann* [2009, 2010] and *Farnetani et al*. [2012] show that such bilateral zoning can be produced by large-scale isotopic differences in the source region of the Hawaiian plume at the base of the mantle. *Weis et al*. [2011] and *Huang et al*. [2011] related this large-scale isotopic structure to the northern edge of the Large Low Shear Velocity Province (LLSVP) at the base of the sub-Pacific mantle [*Romanowicz and Gung*, 2002; *Panning and Romanowicz*, 2006; *Ritsema et al*., 2011]. *Huang et al*. [2011], *Chauvel et al*. [2012], and *Payne et al*. [2013] extended this relationship to other double volcanic chains in the Pacific (Samoa, Marquesas, and Society Islands). A more general geographic association of mantle plumes with the edges of long-lived LLSVPs has been demonstrated by *Burke et al*. [2008]. This lends credibility to the postulate of large-scale compositional gradients near the base of the mantle, where they would be readily sampled by rising mantle plumes.

[5] A fundamentally different approach, originally proposed by *Sleep* [1984], and later elaborated by *Phipps Morgan and Morgan* [1999] and by *Ito and Mahoney* [2005], considers the mantle as an intimate mixture of depleted peridotite, recycled crust in the form of eclogite and/or pyroxenite, and possibly an additional enriched form of (metasomatized?) peridotite. The eclogite/pyroxenite or hydrous peridotite components have lower melting temperatures [e.g., *Hirschmann and Stolper*, 1996; *Yaxley*, 2000], are relatively enriched in incompatible elements, and have higher $^{87}Sr/^{86}Sr$ and lower $^{143}Nd/^{144}Nd$ ratios than the peridotite matrix. *Sleep* [1984] proposed that if small (<5 km) enriched, low-melting "blobs" are homogeneously distributed in the mantle, then their preferential melting beneath a thick lithosphere will yield systematically enriched basalts, relative to ocean-ridge basalts formed in the absence of a lithospheric lid. Geochemical data consistent with this idea include the observation that the most "depleted" isotopic signatures found in hotspot basalts occur when they erupt on or near mid-ocean ridges (Iceland, Galapagos, Ninety-East Ridge near the SE Indian Ridge, and Detroit Seamount on the Emperor ridge [*Class et al*., 1993; *Regelous et al*., 2003; *Huang et al*., 2005; *Frey et al*., 2005; *Sobolev et al*., 2007; *Haase et al*., 2011]). On the other hand, there is also ample evidence that large-scale, mappable isotopic differences do exist in the mantle [e.g., *Hofmann*, 2003; *Davies*, 2009]. Indeed, from our understanding of mantle convection, there are good reasons to think that mantle heterogeneities exist on many length scales [*Davies*, 2002]. Consequently, any discussion of one of the above models to the exclusion of the other is likely to miss important features of the real mantle.

[6] Here we address the question whether small scale (≪5 km) heterogeneities within the Hawaiian plume, the existence of which we do not question, can explain (1) the contrasting isotopic and chemical compositions of the two parallel volcanic chains of the Hawaiian Islands, known as the "Kea-trend" and "Loa-trend" volcanoes (see Figure 1), and (2) the isotopic evolution of individual volcanoes from tholeiitic shield phases to late, alkalic, rejuvenated phases. Such shallow-mantle melting control has been proposed by *Bianco et al*. [2008, 2011] and by *Ballmer et al*. [2011], although *Bianco et al*. [2011] acknowledged that this model cannot explain all of the isotopic heterogeneity of Hawaiian volcanoes. Their "uniformly heterogeneous" model, from now on called "plum pudding" model, implies an efficient mantle mixing that eliminates large-scale compositional zoning. Our objective is to test predictions of the plum pudding model and to critically evaluate the assumption that the Hawaiian plume conduit lacks any geochemical zonation.

[7] First, we use La/Yb as a tracer of melt fraction, because La is incompatible and varies inversely with the melt fraction, whereas Yb is nearly constant in Hawaiian basalts due to garnet buffering in the melting region. This enables us to test whether predictions of lower melt fractions on the Loa side [*Ballmer et al*., 2011] are supported by observations. We then show that the change in melt fraction, which occurs during the transition from shield to postshield phases, has no significant impact on the lead isotopic signature that separates Kea- from Loa-track volcanoes. Finally, we consider the rejuvenated phase of volcanism, characterized by highly variable, often very low degrees of melting. Here the plum pudding models predict the greatest contribution from the chemically and isotopically enriched "plums", at least in the later phases of rejuvenation, but actual rejuvenated lavas consistently show the most depleted isotopic signatures.

To explain their origin, we extend our earlier modeling of the Hawaiian plume [*Farnetani and Hofmann*, 2010] to significantly lower melt production rates and argue that rejuvenated Hawaiian magmas originate from the deep (~5 GPa) underside of the plume, 200–400 km far downstream from shield volcanism. This relatively peripheral part of the plume originally formed the upper portion of the lower-mantle thermal boundary layer, which extends into "ambient"-depleted mantle.

[8] Overall, we find that a plume that is uniform on a large-scale, but randomly heterogeneous on a small scale, cannot generate the large-scale systematic isotopic and chemical relationships observed on the Hawaiian Islands. Instead, these heterogeneities must have deeper sources, plausibly rooted in the thermal boundary layer, from which the plume originates.

[9] We emphasize that neither our "deep origin" model nor the "uniformly heterogeneous plum pudding" models have addressed the origin of short-term compositional fluctuations, ubiquitously observed on Hawaii. These almost certainly do require the existence of small-scale source heterogeneities, which are tapped either randomly [*Blichert-Toft et al*., 2003] or periodically with a frequency peak of 10 kyr [*Eisele et al*., 2003]. These short-term fluctuations will require a separate approach to elucidate the dynamics of melt extraction sampling compositionally distinct heterogeneities [*Spiegelman and Kelemen*, 2003]. Our focus instead will be on the larger-scale, longer-term, compositional features exhibited by the overall evolution of single Hawaiian volcanoes and on the systematic differences between the two parallel volcanic chains.

2. The Plum Pudding Models

[10] According to *Bianco et al*. [2008], a uniform mixture of enriched and depleted peridotite in the Hawaiian conduit generates geochemically distinct volcanic chains because the Loa- and Kea-tracks sample the plume center and the periphery, respectively. The enriched component ("EC") is assumed to be a hydrous peridotite enriched in incompatible elements, with a low value of ϵ_{Nd} and a lowered solidus. We note that this type of small-scale heterogeneity is unlikely to survive in the mantle very long, because water diffusivity in olivine is predicted to reach or exceed values of $D = 10^{-10}$ m^2 s^{-1} at temperatures above 1500°C [*Demouchy and Mackwell*, 2003]. This corresponds to diffusion distances greater than 1 km in 1 Ga. In the model of *Bianco et al*. [2008], the predicted geochemical differences, expressed as ϵ_{Nd}, are caused by the different melt contributions from enriched and depleted components for the off-axis Kea-track relative to the on-axis Loa-track volcanoes.

[11] ϵ_{Nd} values predicted by *Bianco et al*. [2008] are roughly constant during much of the main shield phase, they increase gradually during late shield phases, and they drop sharply to very low values toward the end of the eruptive cycle, because at that stage only the enriched component produces melts. The authors state that "the very last lavas to erupt reveal the low ϵ_{Nd} compositions predicted at the very downstream edge of the melting zone". The isotopic record of the Mauna Kea drill hole (HSDP), which traces the evolution from shield to postshield stage, does indeed show a gradual increase in ϵ_{Nd}, but it does not show any of the low-ϵ_{Nd} predicted for the end of the cycle. On Mauna Loa, a drop to $\epsilon_{Nd} < 4$ is seen for eruptions younger than 20 ka [*DePaolo et al*., 2001], but recent eruptions have $\epsilon_{Nd} = 5.3 \pm 0.4$ [*Weis et al*., 2011], not significantly lower than older shield lavas. In addition, unlike Mauna Kea, Mauna Loa has not yet reached the end phase of its eruptive cycle and should therefore probably not be used to test this particular prediction. Also, no such sharp drop is seen in any of the other Hawaiian post-shield lavas either. *Bianco et al*. [2008] note that their model, like earlier models describing a concentrically zoned plume, fails to predict the transition from tholeiitic to alkalic magmatism as a volcano evolves from shield to postshield phase. They do not address the observation, illustrated further below in the present paper, that the latest phases of Hawaiian volcanism, the rejuvenated stages, consistently show isotopic compositions of the most depleted source component (DC in their terminology). This directly contradicts their map view of the ϵ_{Nd} composition, in which the "tail end" of magmatism is dominated by EC (blue color in their Figure 2).

[12] A new model by *Ballmer et al*. [2011] invokes the effect of small-scale convective rolls in the asthenosphere on the impinging Hawaiian plume. The asthenospheric rolls thermally erode the oceanic lithosphere and create an underside relief resembling a "washboard", with ridges and grooves aligned parallel to the direction of plate motion. Although the amplitude of this washboard relief is an order of magnitude smaller than the difference between near-ridge and thick-lithosphere melting depths, *Ballmer et al*. [2011] use this relief

to explain the isotopic and chemical differences between the two Hawaiian volcanic trends. Their uniformly heterogeneous plume consists of three components, dry peridotite (DC), hydrous peridotite (HC), and (enriched) pyroxenite (PX), with HC and PX having lower solidi than DC. This model qualitatively predicts not only the "tail" of rejuvenated volcanism but also the more distant rim of arch volcanism. However, this model also predicts that the initially low percentage (30–40%) of enriched pyroxenite contribution to rejuvenated lava compositions rises dramatically (60%) toward the end of rejuvenated magmatism and has extreme values (97%) in arch volcanism. It will be seen below that these predictions are not matched by the observed compositions of rejuvenated and North Arch lavas.

[13] In order to explain the difference between the shield-lava compositions of Loa and Kea-track volcanoes, *Ballmer et al*. [2011] invoke an asymmetry between the lithospheric washboard and the center of the plume, so that the lithospheric relief diverts the larger portion of the plume flow toward the Kea side. This side therefore receives the higher bulk melt flux, coupled with a smaller relative contribution from the pyroxenite plums (at least according to their Figure 3, although the caption states the opposite). This is used to explain why the Kea side, with its smaller relative PX component, has the isotopically more depleted character (higher ε_{Nd}). We will show below that the trace element geochemistry of the Kea-side volcanoes require lower, not higher, bulk melt fractions than those of Loa-side volcanoes.

[14] Finally, *Bianco et al*. [2011] elaborate on their earlier model by discussing a larger range of geodynamic conditions and by introducing a third component (dry pyroxenite). For Nd isotopes, their results are similar to *Bianco et al*. [2008]; however, for Pb isotopes, the authors recognize that they cannot explain lead isotope differences between Kea and Loa trends, which instead require zonation of the plume conduit [*Abouchami et al*., 2005; *Farnetani et al*., 2012].

3. Melt Fluxes, Melt Fractions, and La/Yb Ratios

[15] We use La/Yb ratios to evaluate relative bulk-melt fractions. La is a proxy for any of the highly incompatible elements whose abundance in the melt, relative to the source, varies inversely with melt fraction. In contrast, Yb is buffered by garnet during partial melting, but varies in response to fractional crystallization. Thus in general, as melt fraction decreases, La/Yb increases. In the plum pudding models, a decrease in bulk melt fraction causes the relative contribution of the enriched, low-melting temperature, source components to increase. Since these components are assumed to be incompatible-element enriched, their increased contribution will also cause an increase in La/Yb.

[16] *Ballmer et al*. [2011] use the washboard aspect of their lithosphere to explain the difference between the Kea and Loa-trend volcanoes. They predict that Kea-trend volcanoes should have a greater melt flux and bulk melt fraction, and a lower relative proportion of pyroxenite component than Loa-trend volcanoes. Although this prediction is consistent with the higher ϵ_{Nd} values seen in Mauna Kea shield basalts, it should also yield lower La/Yb ratios in Kea-track than Loa-track shield basalts. Figure 2 shows that the opposite is the case: Loa-track shield tholeiites have not only lower $^{143}Nd/^{144}Nd$ (expressed in Figure 2 as ϵ_{Nd}) but also distinctly lower average La/Yb values than Kea-track shield tholeiites. Note that the La/Yb ratio of the various source components cannot be assumed to be identical. However, La/Yb is expected to be positively correlated with Nd/Sm. The enriched source components are thus characterized by relatively high La/Yb and Nd/Sm, but low $^{143}Nd/^{144}Nd$. At a given melt fraction, an increased contribution by such a component will produce melts with relatively high La/Yb and low $^{143}Nd/^{144}Nd$. In the case at hand, the Loa-track volcanoes have systematically lower $^{143}Nd/^{144}Nd$ ratios than the neighboring Kea-track volcanoes, but they also have lower, rather than higher, La/Yb ratios. Therefore, Loa-track volcanoes must have significantly higher melt fractions, which must have overcompensated their higher source-La/Yb ratios. Thus, in the particular case of Hawaiian shield volcanoes, the inverse relation between melt fraction and melt-La/Yb can be used as a reliable indicator of *relative* melt fractions.

[17] Figure 3 shows that, with one exception, melt fractions are systematically different for essentially the entire double chain back to Molokai: The averages for four Loa-trend shields (Mauna Loa, Hualalai, Lanai, Kahoolawe) and six Kea-trend shields (Kilauea, Mauna Kea, Kohala, Haleakala, West Maui, East Molokai) demonstrate that nearly all Kea-trend shields have consistently higher La/Yb ratios than Loa-trend shields. The

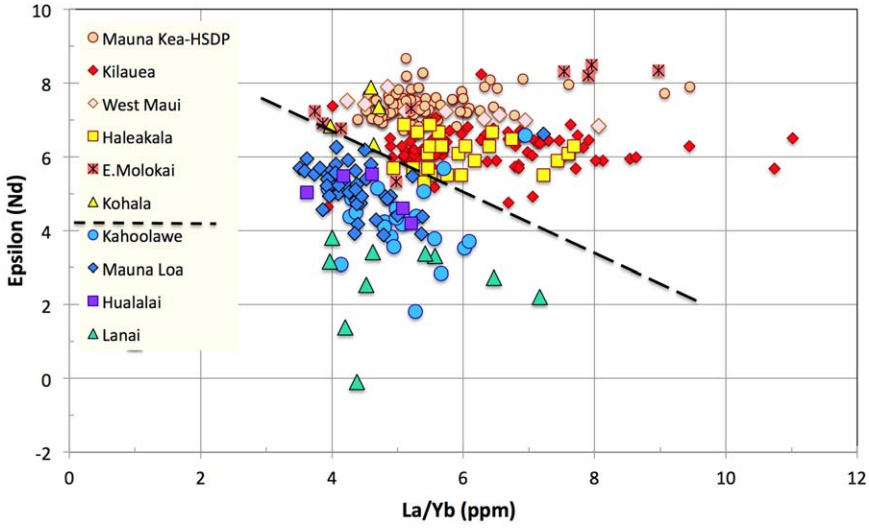

Figure 2. La/Yb ratios versus ϵ_{Nd} (both in ppm) for shield stage lavas of Loa-trend volcanoes (cool color symbols) Mauna Loa, Hualalai, Lanai, and Kahoolawe, and Kea-trend volcanoes (warm color symbols) Kilauea, Mauna Kea, Kohala, Haleakala, West Maui, and East Molokai. Data for Mahukona and West Molokai are omitted for reasons explained in the text. Data sources are given in supporting information.[1]

single exception is Kohala, which has a La/Yb average essentially identical to Kahoolawe. (Note that we have not plotted data for West Molokai, because its location cannot be clearly associated with either the Loa or the Kea track, and for Mahukona, because it is isotopically exceptionally heterogeneous, and its geology, including the location of its summit, is disputed in the literature [*Clague and Moore*, 1991; *Garcia and Kurz*, 1991]). In conclusion, the observed La/Yb ratios indicate that melt fractions are higher in Loa-trend than in Kea-trend shield-phase melts, contrary to one of the basic assumptions of the model by *Ballmer et al*. [2011].

4. Model Predictions Versus Observed Lead Isotopes

[18] *Abouchami et al*. [2005] showed that Pb-isotopic compositions provide the "cleanest" discriminant between Loa and Kea-track volcanoes, and this has been borne out by subsequent additional work on both shield-phase and postshield phase basalts from the two tracks [*Hanano et al*., 2010]. The main exceptions are West Molokai and Mahukona, which contain both Kea-type and Loa-type Pb isotopes (*Xu et al*. [2007], their Figure 10). For reasons noted above, these volcanoes will not be further discussed here. All of the schemes employing small-scale heterogeneities to explain the observed systematic isotopic distinctions ultimately rely on invoking preferential sampling of

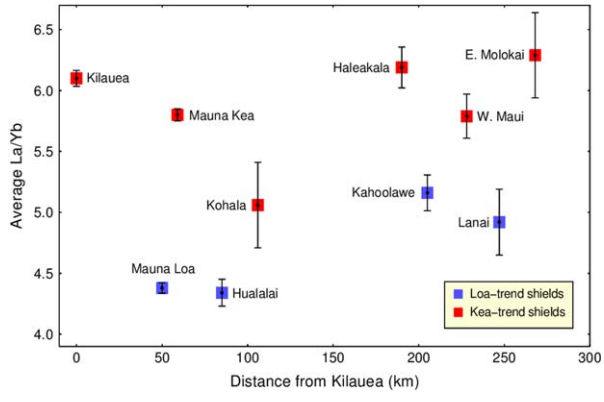

Figure 3. Distance with respect to Kilauea versus average La/Yb (ppm) values and standard errors of four Loa-track volcanoes (blue) and six Kea-track volcanoes (red). These data reveal consistently lower degrees of melting/higher pyroxenite contributions in Kea-track than in Loa-track volcanoes, contrary to the prediction of *Ballmer et al*. [2011]. Kohala represents the only overlap in these averages. For each volcano we provide the number of samples, the average La/Yb, the standard deviation: Kilauea (245; 6.1; 1.03), Mauna Loa (156; 4.38; 0.54), Mauna Kea (199; 5.8; 0.72), Hualalai (14; 4.34; 0.42), Kohala (20; 5.06; 1.6), Haleakala (43; 6.19; 1.1), Kahoolawe (28; 5.16; 0.78), West Maui (29; 5.79; 0.98), Lanai (13; 4.92; 0.99), East Molokai (29; 6.29; 1.91). Data sources are given in supporting information.

[1]Additional supporting information may be found in the online version of this article.

isotopically and chemically distinct components in response to variations in bulk melt fraction. We have shown above that bulk melt fractions differ systematically between the two tracks. We now focus on the evolution of individual volcanoes on either of these tracks.

[19] The Pb isotopes conventionally plotted on a $^{208}Pb/^{204}Pb$ versus $^{206}Pb/^{204}Pb$ can be conveniently expressed by a single parameter, namely

$$^{208}Pb^{*}/^{206}Pb^{*} = \frac{(^{208}Pb/^{204}Pb)_{sample} - (^{208}Pb/^{204}Pb)_{pr}}{(^{206}Pb/^{204}Pb)_{sample} - (^{206}Pb/^{204}Pb)_{pr}} \quad (1)$$

known as the "radiogenic $^{208}Pb/^{206}Pb$ ratio" [*Galer and O'Nions*, 1985], where the primordial (pr) values we used are from *Blichert-Toft et al*. [2010]. Alternatively, one can use Hart's [*Hart*, 1984] purely empirical parameter Δ8/4, the deviation from the so-called Northern Hemisphere Reference Line (NHRL) defined as

$$(^{208}Pb/^{204}Pb)_{NHRL} = 1.209\ (^{206}Pb/^{204}Pb)_{NHRL} + 15.627 \quad (2)$$

so that

$$\Delta 8/4 = 100[(^{208}Pb/^{204}Pb)_{sample} - (^{208}Pb/^{204}Pb)_{NHRL}]. \quad (3)$$

[20] Note that $^{208}Pb^{*}/^{206}Pb^{*}$ is afflicted by significant error magnification because the difference between the present-day and the primordial $^{208}Pb/^{204}Pb$ ratios is only about half the present-day value. This leads to excessive scatter in many older sets of measurements where variable instrumental mass fractionation was poorly controlled. This is the main reason why the remarkable distinction in Pb isotopes between the two Hawaiian volcano tracks was rather blurred in older publications.

[21] Figure 4a shows that, for Hawaiian basalts, the parameters $^{208}Pb^{*}/^{206}Pb^{*}$ and Δ8/4 are tightly correlated and can be used virtually interchangeably. Both parameters are consistently higher in Loa-track than in Kea-track volcanoes, and this is true for both shield and postshield phases. Figure 4b, plotting $^{208}Pb^{*}/^{206}Pb^{*}$ versus La/Yb, shows in more detail that the preshield (Loihi) and postshield phases do not systematically differ in their isotopic compositions from shield phases within each trend. The consistent difference of isotopic compositions between the two tracks, and the absence of such a difference as a result of changing melt fractions, provides the strongest argument that these isotopic compositions represent larger-scale differences in plume composition rather than small-scale, "plum pudding" heterogeneities. We infer from the above that the differences in lead isotopes between Loa and Kea chains must be derived from a deeper source, and this was in fact acknowledged by *Bianco et al*. [2011]. We emphasize that we do not rule out the possibility that differential melting of small-scale heterogeneities may affect the chemical and isotopic compositions of the erupted lavas. Indeed, this may well explain many or all of the short-term fluctuations of isotopic composition observed within the HSDP (Hawaiian Scientific Drilling Project) drill core [*Bianco et al*., 2011], as well as in the historic record of Mauna Loa and Kilauea eruptions. However, on the larger spatial scale of the systematic Loa-Kea differences, and on the longer temporal scale from preshield to postshield phases, these effects are overwhelmed by a larger-scale zonation of the plume conduit.

5. Rejuvenated Volcanism

[22] The phenomenon of rejuvenated volcanism, which occurs on many Hawaiian volcanoes after an eruptive hiatus of up to 2 m.y., is among the least understood and most controversial aspects of Hawaiian volcanism. These lavas are small in volume and variably alkaline (sometimes nephelinitic) in chemical composition, but their isotopic signatures consistently indicate derivation from depleted sources. They were once widely believed to be derived from the oceanic lithosphere that had been heated by the Hawaiian plume [e.g., *Chen and Frey*, 1985; *Gurriet*, 1987]. More complete isotope data accumulated in the recent literature have shown, however, that there are systematic differences between these signatures and those found on the East Pacific Rise and in the Pacific crust near Hawaii. Thus, it appears that the sources of rejuvenated magmas must be found in the plume itself [*Frey et al*., 2005; *Fekiacova et al*., 2007; *Garcia et al*., 2010].

[23] In the models of *Bianco et al*. [2008, 2011] and *Ballmer et al*. [2011], melts in the outermost region of the Hawaiian melting zone are increasingly derived from the enriched component(s) (pyroxenite and/or enriched peridotite). *Ballmer et al*. [2011] explicitly predict X_{PX}, the proportion of enriched-component-derived melt, as a function of distance along the volcanic track. They find that X_{PX} is low (~30%) at the onset of rejuvenated magmatism, but increases toward ~60% at the

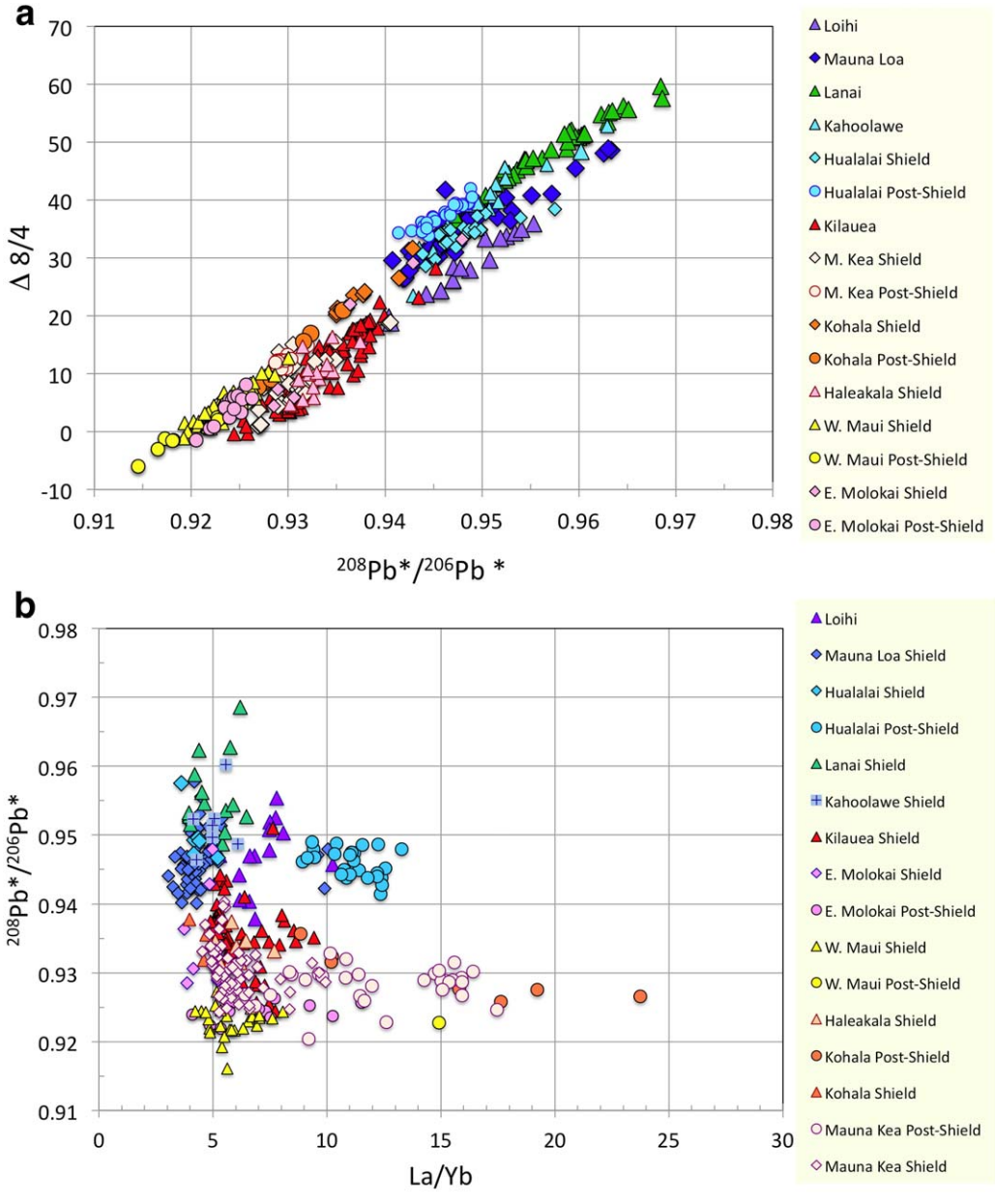

Figure 4. (a) $^{208}Pb^*/^{206}Pb^*$ (radiogenic $^{208}Pb/^{206}Pb$ ratio) versus Δ8/4 (deviation of $^{208}Pb/^{204}Pb$ from Hart's Northern Hemisphere Reference Line; see text for definitions of both parameters) for preshield lavas from Loihi, shield lavas from Mauna Loa, Hualalai, Lanai, Kahoolawe, Kilauea, West Maui, Haleakala, Kohala, and Mauna Kea, and for postshield lavas from Hualalai, West Maui, Kohala and Mauna Kea. The two parameters are strongly correlated and both are proxies for Th/U ratios of the magma sources. Loa-track volcanoes have consistently higher $^{208}Pb^*/^{206}Pb^*$ ratios than Kea-track volcanoes. Preshield Loihi lavas have indistinguishable $^{208}Pb^*/^{206}Pb^*$ ratios from shield-phase Mauna Loa lavas, showing that the lower degree of melting of preshield magmas does not significantly affect $^{208}Pb^*/^{206}Pb^*$ ratios. The same is true for postshield phases of both Loa and Kea-track volcanoes. (b) La/Yb versus $^{208}Pb^*/^{206}Pb^*$ comparing shield and postshield phases of Hawaiian volcanoes. The diagram shows that postshield lavas are characterized by higher La/Yb ratios, and therefore lower melt fractions, than corresponding shield lavas, but their isotopic compositions are similar. Data sources are given in supporting information.

end, whereas values are >97% in arch volcanism. In general, therefore, this model predicts highly variable and increasingly enriched isotopic signatures. However, *Ballmer et al*. [2011] note that the material erupted during rejuvenated and arch magmatism is derived from the peripheral part of the

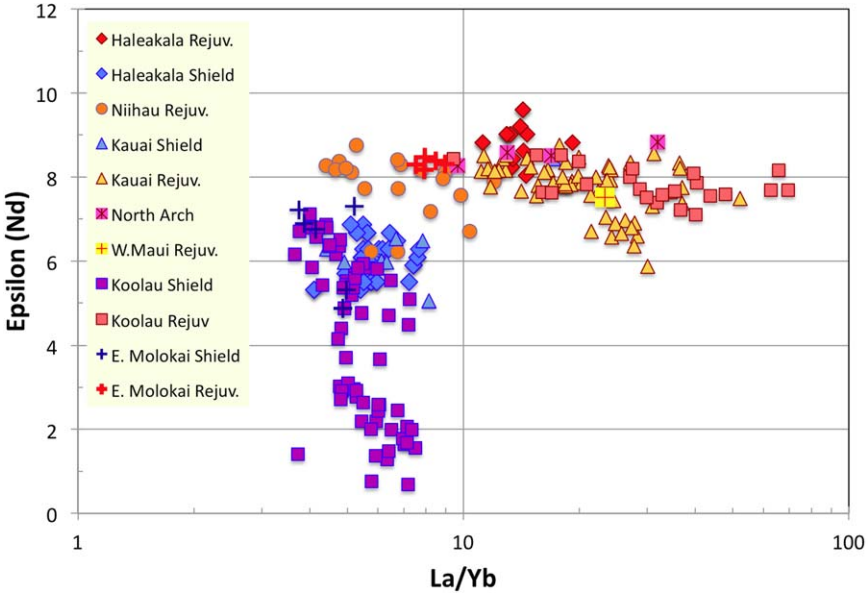

Figure 5. La/Yb versus ϵ_{Nd} for shield and rejuvenated lavas from six Hawaiian volcanoes and for the North Arch Volcanic Fields. For rejuvenated and North Arch lavas (warm color symbols), La/Yb ratios are high but highly variable, ϵ_{Nd} values are rather uniformly high. For shield lavas (cold color symbols), La/Yb ratios are relatively uniform, and ϵ_{Nd} values are rather variable. Data sources are given in supporting information.

conduit which may contain isotopically more depleted material, derived by entrainment from ambient upper mantle.

[24] Figure 5 shows the available Nd isotope data for rejuvenated lavas from six Hawaiian volcanoes, plus four samples from the North Arch, believed to be an off-axis form of rejuvenated volcanism. ϵ_{Nd} is plotted here as a function of La/Yb for the rejuvenated lavas and corresponding shield lavas from the same volcanoes. La/Yb ratios are high and highly variable in rejuvenated lavas, and relatively uniform in shield lavas. In contrast, ϵ_{Nd} values are rather variable, at least in some shield volcanoes, and rather uniformly high in all rejuvenated eruptions. Another important observation, noted by *Hanano et al*. [2010] and by *Garcia et al*. [2010], is that the distinction between Loa-track and Kea-track isotopic compositions is lost in the rejuvenated phases. Figure 5 shows that the rise in enriched source component predicted by *Ballmer et al*. [2011] is not observed in any of the six rejuvenated suites and especially not in the North Arch lavas, predicted to contain >97% enriched source component. All four published North Arch values of $\epsilon_{Nd} > 8.0$ indicate source materials that are among the isotopically most depleted anywhere within the Hawaiian suite of basalts. Unpublished data on a larger suite of Arch basalts have confirmed this observation (Hanan, Personal Communication May 2013).

[25] We conclude that models calling on differential melting of small-scale heterogeneities explain neither the systematic isotopic differences between Loa and Kea-volcanic tracks nor the depleted-source character of all observed rejuvenated volcanism.

[26] Other authors have attempted to explain the nature of rejuvenated volcanism in a variety of ways. For example, *Frey et al*. [2005] suggest that the source material of rejuvenated magmas is a depleted component intrinsic to the plume, and *Fekiacova et al*. [2007] speculate that such a component is incorporated in the outer margin of the plume by entrainment of "ambient" depleted mantle during its ascent. *Bianco et al*. [2005] suggest that lithospheric flexure induces secondary melting, whereas *Garcia et al*. [2010] propose a hybrid model involving both lithospheric flexure and a second stage of melting of depleted, but recently reenriched plume components, without specifying what might cause the reenrichment. *Dixon et al*. [2008] invoke carbonatite metasomatism to enrich the outer portion of the Hawaiian plume, in order

to explain the extreme enrichments of Sr and Ba observed in rejuvenated basalts from Niihau. However, recent work by *Dasgupta et al*. [2009] on trace element partitioning between carbonatite melt and garnet lherzolite is inconsistent with the anomalous Ba and Sr abundances at Niihau, a feature which is not observed in other rejuvenated volcanoes, such as Kauai or Koolau.

[27] How can we reconcile the robust observations of relatively uniform, depleted, but unlike-Pacific-MORB isotopic compositions, combined with high but variable enrichments of incompatible elements shared by all rejuvenated Hawaiian lavas? Note that, in addition to the general enrichment of highly incompatible elements, these melts are generally not volatile depleted. It therefore seems quite unlikely that they are derived from a part of the plume from which melt has already been extracted during the main shield and postshield phases.

5.1. A Model for Rejuvenated Volcanism

[28] Pioneering simulations of the Hawaiian plume by *Ribe and Christensen* [1999] found that primary melting feeding the shield phases is followed, 300–500 km downstream, by secondary, rejuvenated, melting. However, two-stage melting models have difficulties in explaining geochemical observations, as discussed above. Here we use and extend our model of the Hawaiian plume [*Farnetani and Hofmann*, 2010] to investigate the depth and origin of rejuvenated magmatism. To familiarize the reader with this model, we briefly summarize its main features: The plume buoyancy flux is $B = 6400$ kg s^{-1}, a value in the range of estimates by *Davies* [1988] and by *Sleep* [1990] (i.e., 6200 and 8700 kg s^{-1}, respectively). The imposed plate velocity is $v_x = 9$ cm/yr, the plume excess temperature is $\Delta T = 250$°C, and we calculate the solidus temperature of anhydrous peridotite following *Katz et al*. [2003]. We also calculate three dimensional flow trajectories within the melting zone and assume a constant melt productivity ($dF/dP = 0.8$ wt% kbar^{-1}) along each trajectory. Finally, we assume that melting stops once the cumulative melt production sums up to 10 wt%. In the following, we use exactly the same model, but extend it to the significantly lower melting rates occurring far downstream from shield volcanism.

[29] Figure 6 shows that the melting zone feeding the preshield, shield, and postshield phases is characterized by high melting rates ($1 < \Gamma < 8 \times 10^{-11}$ kg m^{-3}s^{-1}), whereas the melting rate is much lower ($0.01 < \Gamma < 1 \times 10^{-11}$ kg m^{-3}s^{-1}) far downstream where rejuvenated volcanism occurs. Note that low values reflect decreasing upwelling velocities, since

$$\Gamma = v_z \rho^2 g (dF/dP) \tag{4}$$

where v_z is vertical velocity, ρ is mantle density, g is gravitational acceleration and dF/dP is melt productivity. The low values of Γ, observed far downstream, reflect low (but greater than zero) upwelling velocities. Contrary to *Ribe and Christensen* [1999] we do not find a region of downgoing flow and the consequent melt shut off 200–300 km downstream. In Figure 6, the lowermost red dot on each melting trajectory marks the beginning of melting (i.e., $F = 0$). Each 1% increment in ΔF is marked by an additional red dot. Far downstream, the locus of rejuvenated magmatism, the upper portion of the melting region still produces melt, which is however severely depleted in incompatible elements including Nd, Hf, Sr, and Pb, because this material has already lost significant amounts of melt during the shield and postshield phases. This is a consequence of the rapid extraction of incompatible elements during the first 1–2% of fractional or continuous melting. Therefore, only the lowermost part of the plume, which crosses the solidus at ~150 km depth, is capable of producing melts that are enriched in incompatible elements, and these bear the isotopic compositions of relatively peripheral parts of the plume. This portion of the plume is still fertile with regard to incompatible elements, since it has not been subjected to previous melt extraction (see trajectories in Figure 6).

[30] Figure 7 shows the local, incremental, extent of melting ΔF, the cumulative mean melt extent $\overline{F}$, and the melt production rate M, all calculated within a 30 km radius magma capture zone beneath a central volcano. The cumulative mean melt extent is

$$\overline{F} = \frac{\int \Gamma F dV}{\int \Gamma dV} \tag{5}$$

where V is volume. In Figure 7, the maxima for the melt production rate M and for the local extent of melting do not coincide because M is proportional to the vertical velocity (since $M = \int (\Gamma / \rho_{melt}) dV$), whereas the local extent of melting ΔF is proportional to the slope of the trajectory (i.e., $F = 10$ wt% for a vertical trajectory and $F = 0$

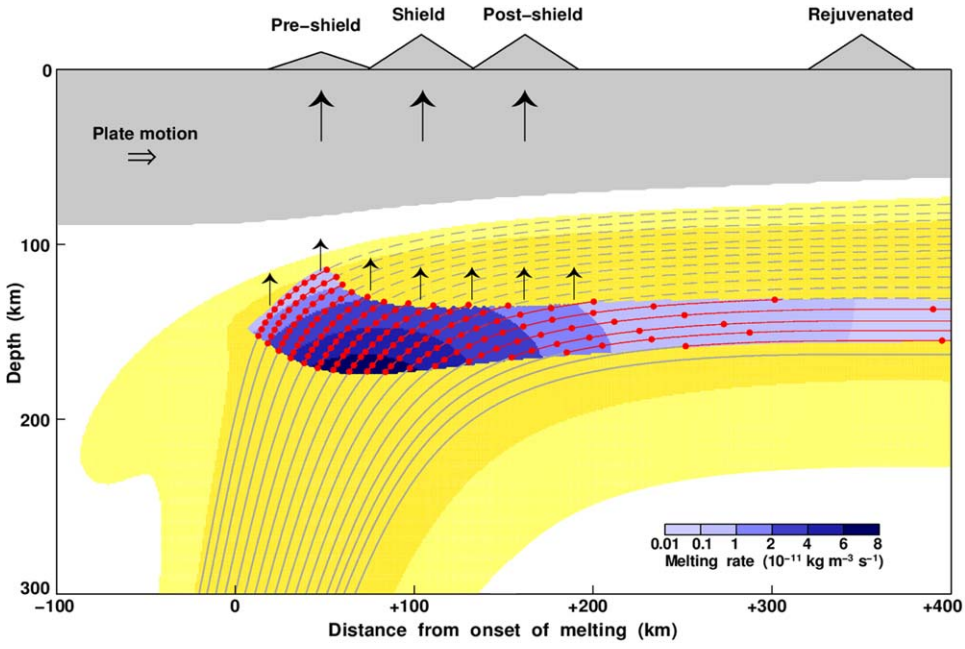

Figure 6. This figure is based on the numerical modeling of *Farnetani and Hofmann* [2010], but extended to depict regions containing much lower melting rates ($\Gamma < 1 \times 10^{-11}$ kg m^{-3} s^{-1}). Solid trajectories are shown before melting (grey lines), during melting (red lines, with dots for each additional 1 wt% melt produced), and once the peridotitic restite becomes too refractory to undergo additional melting (dashed lines). Note that the first red dot on each melting trajectory marks the beginning of melting ($F = 0$). Melting is assumed to stop at $F = 10\%$. Far downstream, the only fertile trajectories are from the underside part of the plume, and we predict that rejuvenated melts originate at 150–130 km depth.

wt% for a horizontal one), and thus depends on both vertical and horizontal velocity components. The cumulative mean melt extent $\overline{F}$ shows an initial maximum during the shield phase, a small decrease during the postshield phase, and a gradual increase during the rejuvenated phase. The reason for this is that, under our rather simplistic assumption for the pressure dependence of the melt production ($dF/dP = 0.8$ wt% kbar^{-1}), the upper portion of the melting region continues to contribute melt increments with cumulative values up to 10%, thus yielding $\overline{F}$ values of about 5%, so that incompatible elements should actually be slightly less enriched in the rejuvenated melts than in the tholeiites formed during the shield and postshield phases. This melting and melt extraction scheme is therefore roughly consistent with the rather low (5–10) values of La/Yb seen in Niihau and West Maui rejuvenated lavas (Figure 5) but not with the much more enriched La/Yb ratios (up to 80) found on other rejuvenated volcanoes. This model also cannot explain the high variability of La/Yb in these rejuvenated lavas. *Bianco et al.* [2008] encountered the same problem and concluded that it "presents a new challenge for all dynamical models of plume-plate interaction to explain". To escape this conundrum, we speculate that, perhaps because of the very low overall melting rates, some of these melts are extracted directly from the lowermost part of the melting region, without interaction with the overlying parts of the melting region. This speculation is consistent with the observation that for Kauai rejuvenated lavas, the samples with the lowest CaO content, for which *Garcia et al.* [2010] determined relatively low pressures of equilibration (3.5–4.0 GPa), also have the lowest La/Yb ratios. Separate extraction of melts from different depths in this region is also consistent with the existence of nanodiamonds in Salt Lake Crater garnet pyroxenites from Oahu [*Wirth and Rocholl*, 2003; *Frezzotti and Peccerillo*, 2007] and with petrologic evidence that some pyroxenites carried by rejuvenated lavas crystallized at depths of up to 150 km [*Keshav et al.*, 2007], whereas other estimates of crystallization pressures [e.g., *Bizimis et al.*, 2005] of Salt Lake Crater pyroxenites range only between 2 to 3 GPa, even lower than the equilibration pressures estimated by *Garcia et al.* [2010]. We emphasize that, independent of the degree of

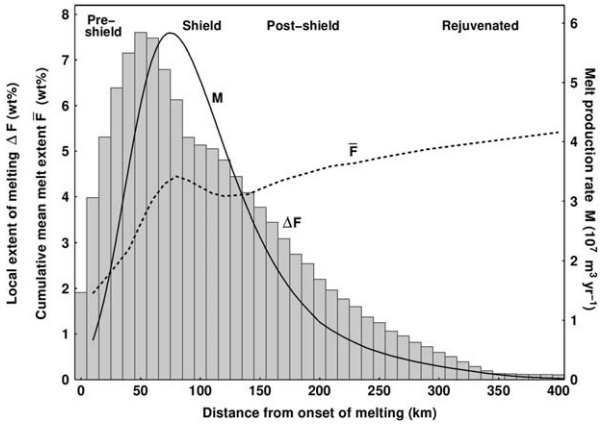

Figure 7. Local extent of melting ΔF (histogram), cumulative mean melt extent $\overline{F}$ (dashed line), and melt production rate M (solid line), all calculated within a cylindrical magma capture zone of 30 km radius and plotted versus distance. The high values of $\overline{F}$ in the rejuvenated region are an outcome of the very simple melting and melt extraction model assumptions, and are contradicted by the highly variable and commonly very low $\overline{F}$ of rejuvenated melts required by geochemical observations [see also *Bianco et al*., 2008].

"dilution" of the melt by melt increments originating in the upper portion of the downstream apron of the plume, the incompatible-element budget (including Sr, Nd, Hf, Pb) of the erupted melts will be almost quantitatively derived from the plume's lowermost portion, which has not undergone previous melting and melt extraction. Therefore, the isotopic compositions of these elements will also reflect primarily that same lowermost "underbelly".

[31] The question remains whether the underside of the plume is ambient mantle, incorporated into the plume by entrainment during ascent, or whether it is lower mantle material from the thermal boundary layer. By using the parameterization for anhydrous melting by *Katz et al*. [2003], the solidus temperature at 150 km depth (i.e., $P \sim 4.8$ GPa) is $T = 1610°C$, which means a potential temperature $\theta \sim 1520°C$, roughly 200°C hotter than the commonly assumed $\theta_{mantle} \sim 1320°C$. Ambient mantle entrained during plume ascent is unlikely to attain such a high excess temperature. Instead, we posit that this material is part of the normal plume conduit, plausibly situated at an intermediate radius between the hottest core and the coldest rim. (Note that the relation between real and potential temperature is given by $\theta = T\exp(-g\alpha d/C_p)$, where α the thermal expansion coefficient, d is depth and C_p the specific heat).

[32] Following *Farnetani and Hofmann* [2009], we show a simple example of a large-scale geochemical zonation in the thermal boundary layer (TBL) that would generate a bilateral conduit surrounded by a rim of relatively hot but depleted material (Figure 8, bottom). The deepest part of the TBL, with Kea-type material (red) to the North and Loa-type (blue) to the South, is overlain by a layer (green) which has the composition of ordinary deep-mantle material, now widely recognized

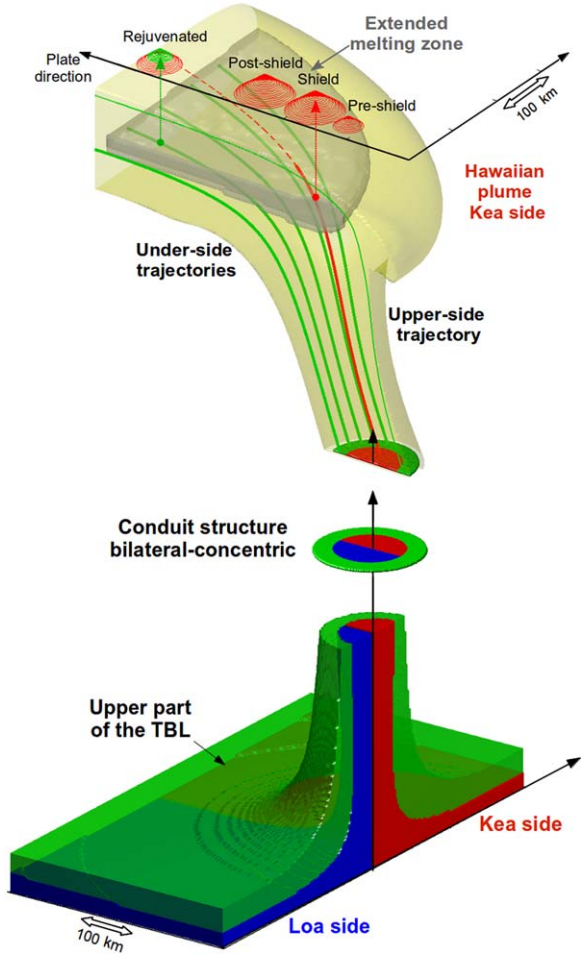

Figure 8. (bottom) Geochemical zonation across the thermal boundary layer (TBL) that generates a bilateral conduit (red for the northern Kea-side, blue for the southern Loa-side) surrounded by a peripheral rim of relatively depleted material (green), originally located in the upper part of the TBL. Note that colors are used to schematically represent material with distinct isotopic fingerprint. (top) Numerical simulation of the Hawaiian plume, only the Kea-side is shown. Colored 3-D surfaces for constant excess temperature (yellow) and for the extended melting zone (gray). Green lines are calculated trajectories from the peripheral rim of depleted material, more specifically, five downstream trajectories from the under-side of the plume and one upstream trajectory from the upper-side. The red line is a trajectory from the central (Kea) part of the conduit, before and during melting (solid line), after melting (dashed line).

to be rather depleted, either as a result of the segregation of a very early enriched reservoir [*Boyet and Carlson*, 2005] or, alternatively, because the Earth is generally more depleted in incompatible elements than average chondrites [*Caro and Bourdon*, 2010; *O'Neill and Palme*, 2008].

[33] The "bilateral-concentric" conduit structure, shown in Figure 8, is then used in the numerical simulation of the Hawaiian plume, so that we can calculate the flow trajectories within the stem and in the melting zone. Flow trajectories from the depleted (green) upstream part of the plume conduit (Figure 8, top) show that this material undergoes some partial melting during the preshield phase of volcanism, but these melts are mixed with, and thus diluted by, melts rising from more central portions of the plume which contain "blue" or "red" Loa or Kea-track source rocks (see also Figure 6). The situation after cessation of the postshield volcanism is very different. At this point, the melts that continue to be formed from the inner part of the plume are depleted in incompatible elements, leaving only the peripheral region on the downstream underside of the plume to contribute incompatible elements and their isotopes.

[34] The above simple model provides a framework to explain simultaneously (1) the bilateral zonation observed in pre-shield, shield, and postshield stages of Kea and Loa-trend volcanoes, (2) the enigmatic isotopically depleted nature of rejuvenated lavas, and (3) the lack of Kea-Loa distinction far downstream.

6. Conclusion

[35] The shallow-mantle processes invoked by the "uniformly heterogeneous plum pudding" models fail two simple geochemical tests, the distribution of La/Yb ratios of shield-phase basalts, and the mapping of $^{208}Pb^*/^{206}Pb^*$ ratios in preshield, shield, and postshield-phase Hawaiian basalts. In addition, all plum pudding models predict melting to be dominated by the enriched plums toward the end of the life of each volcano. This prediction is contradicted by the isotopically depleted nature of rejuvenated volcanism. Instead, we propose that the source material of rejuvenated melting and volcanism is derived from the upper portion of the lower-mantle thermal boundary layer. This material consists of ordinary depleted mantle, which lies above the region containing the specifically Loa and Kea-like source components that dominate the shield phases. The source material of rejuvenated melting is most likely similar in composition to average depleted mantle, as proposed by recent bulk-Earth models, and it forms the peripheral, relatively hot, rim around the bilaterally zoned conduit center. Our numerical simulation of the Hawaiian plume focused on the melts formed 200–400 km downstream from the locus of shield volcanism. Far downstream, previously unmelted material from the peripheral part of the conduit slowly rises and crosses the solidus at ~5 GPa, generating low melt fractions of rejuvenated magmas. These melts reflect the isotopic signatures of incompatible elements from the outer part of the plume, although the initial chemical enrichment of these elements is lost if these "low-F" melts mix with the highly depleted melts still being formed higher up in the melting region. This model can therefore resolve previously unexplained features of rejuvenated lavas, in particular the lack of Kea-Loa distinction, and their enigmatic isotopic nature. However, more realistic melt extraction modeling will be required to explain quantitatively the problem originally posed by *Bianco et al*. [2008], namely how the very low melt fractions characterizing many rejuvenated lavas reach the surface.

[36] Although shallow-level processes very likely account for the short-term compositional fluctuations observed at Hawaii and other hotspots, their effects do not obscure the isotopic source differences inherited from a deep thermal boundary layer at the base of the Hawaiian plume. This is consistent with the observed correlations between plume geochemistry and deep-mantle seismic tomography as well as with dynamic modeling of deep-mantle plumes.

Acknowledgments

[38] We thank Fred Frey and Mike Garcia for discussions and Barry Hanan for informally confirming the range of published Nd isotopic compositions of North Arch lavas with new, unpublished data. We acknowledge extensive use of the GEOROC database for finding and extracting geochemical data for Hawaiian volcanoes. We thank Garrett Ito, Francis Albarède, Ross Kerr and an anonymous reviewer for their thorough and constructive reviews, and Janne Blichert-Toft for her efficient editorial handling. We are particularly grateful to Garrett Ito for saving us from committing a serious blunder in our discussion of the relevant melt fractions during rejuvenated magmatism. C.G.F. wishes to thank Emmeline Mytard and the French Agence National de la Recherche for funding the ANR-10-BLANC-0603 program. LDEO Contribution No. 7747; IPGP Contribution No. 3462.

References

Abouchami, W., A. W. Hofmann, S. J. G. Galer, F. Frey, J. Eisele, and M. Feigenson (2005), Pb isotopes reveal bilateral asymmetry and vertical continuity in the Hawaiian plume, *Nature*, *434*, 851–856.

Ballmer, M. D., G. Ito, J. van Hunen, and P. J. Tackley (2011), Spatial and temporal variability in Hawaiian hotspot volcanism induced by small-scale convection, *Nat. Geosci.*, *4*, 457–460, doi:10.1038/NGEO1187.

Bianco, T. A., G. Ito, J. M. Becker, and M. O. Garcia (2005), Secondary Hawaiian volcanism formed by flexural arch decompression, *Geochem. Geophys. Geosyst.*, *6*, Q08009, doi:10.1029/2005GC000945.

Bianco, T. A., G. Ito, J. van Hunen, M. D. Ballmer, and J. J. Mahoney (2008), Geochemical variation at the Hawaiian hot spot caused by upper mantle dynamics and melting of a heterogeneous plume, *Geochem. Geophys. Geosyst.*, *9*, Q11003, doi:10.1029/2008GC002111.

Bianco, T. A., G. Ito, J. van Hunen, M. D. Ballmer, and J. J. Mahoney (2011), Geochemical variations at intraplate hot spots caused by variable melting of a veined mantle plume, *Geochem. Geophys. Geosyst.*, *12*, Q0AC13, doi:10.1029/2011GC003658.

Bizimis, M., G. Sen, V. J. M. Salters, and S. Keshav (2005), Hf-Nd-Sr isotope systematics of garnet pyroxenites from Salt Lake Crater, Oahu, Hawaii: Evidence for a depleted component in Hawaiian volcanism, *Geochim. Cosmochim. Acta*, *69*, 2629–2646, doi:10.1016/j.gca.2005.01.005.

Blichert-Toft, J., D. Weis, C. Maerschalk, A. Agranier, and F. Albarède (2003), Hawaiian hot spot dynamics as inferred from the Hf and Pb isotope evolution of Mauna Kea Volcano, *Geochem. Geophys. Geosyst.*, *4*(2), 8704, doi:10.1029/2002GC000340.

Blichert-Toft, J., B. Zanda, D. S. Ebel, and F. Albarède (2010), The solar system primordial lead, *Earth Planet. Sci. Lett.*, *300*, 152–163, doi:10.1016/j.epsl.2010.10.001.

Boyet, M., and R. W. Carlson (2005), ^{142}Nd evidence for early (>4.53 Ga), global differentiation of the silicate Earth, *Science*, *309*, 576–581, doi:10.1126/science.1113634.

Bryce, J. G., D. J. DePaolo, and J. C. Lassiter (2005), Geochemical structure of the Hawaiian plume: Sr, Nd, and Os isotopes in the 2.8 km HSDP-2 section of Mauna Kea Volcano, *Geochem. Geophys. Geosyst.*, *6*, Q09G18, doi:10.1029/2004GC000809.

Burke, K., B. Steinberger, T. H. Torsvik, and M. A. Smethurst (2008), Plume generation zones at the margins of Large Low Shear Velocity Provinces on the coremantle boundary, *Earth Planet. Sci. Lett.*, *265*, 49–60.

Caro, G., and B. Bourdon (2010), Non-chondritic Sm/Nd ratio in the terrestrial planets: Consequences for the geochemical evolution of the mantle crust system, *Geochim. Cosmochim. Acta*, *74*, 3333–3349.

Chauvel, C., R. C. Maury, S. Blais, E. Lewin, H. Guillou, G. Guille, P. Rossi, and M. A. Gutscher (2012), The size of plume heterogeneities constrained by Marquesas isotopic stripes, *Geochem. Geophys. Geosyst.*, *13*, Q07005, doi:10.1029/2012GC004123.

Chen, C. Y., and F. A. Frey (1985), Trace element and isotopic geochemistry of lavas from Haleakala Volcano, East Maui, Hawaii: Implications for the origin of Hawaiian basalts, *J. Geophys. Res.*, *90*, 8743–8768, doi:10.1029/JB090iB10p08743.

Clague, D. A., and J. G. Moore (1991), Comment on "Mahukona: The missing Hawaiian Volcano" by M. O. Garcia, M. D. Kurz, and D. W. Muenow, *Geology*, *19*, 1049–1050.

Class, C., S. L. Goldstein, S. J. G. Galer, and D. Weis (1993), Young formation age of a mantle plume source, *Nature*, *362*, 715–721, doi:10.1038/362715a0.

Dasgupta, R., M. M. Hirschmann, W. F. McDonough, M. Spiegelman, and A. C. Withers (2009), Trace element partitioning between garnet lherzolite and carbonatite at 6.6 and 8.6 GPa with applications to the geochemistry of the mantle and of mantle-derived melts, *Chem. Geol.*, *262*, 57–77.

Davies, G. F. (1988), Ocean bathymetry and mantle convection: 1. Large-scale flow and hotspots, *J. Geophys. Res.*, *93*, 10,467–10,480.

Davies, G. F. (2002), Stirring geochemistry in mantle convection models with stiff plates and slabs, *Geochim. Cosmochim. Acta*, *66*, 3125–3142, doi:10.1016/S0016-7037(02)00915-8.

Davies, G. F. (2009), Reconciling the geophysical and geochemical mantles: Plume flows, heterogeneities, and disequilibrium, *Geochem. Geophys. Geosyst.*, *10*, Q10008, doi:10.1029/2009GC002634.

Demouchy, S., and S. Mackwell (2003), Water diffusion in synthetic iron-free forsterite, *Phys. Chem. Miner.*, *30*, 486–494, doi:10.1007/s00269-003-0342-2.

DePaolo, D. J., J. G. Bryce, A. Dodson, D. L. Shuster, and B. M. Kennedy (2001), Isotopic evolution of Mauna Loa and the chemical structure of the Hawaiian plume, *Geochem. Geophys. Geosyst.*, *2*, 1044, doi:10.1029/2000GC000139.

Dixon, J., D. A. Clague, B. Cousens, M. L. Monsalve, and J. Uhl (2008), Carbonatite and silicate melt metasomatism of the mantle surrounding the Hawaiian plume: Evidence from volatiles, trace elements, and radiogenic isotopes in rejuvenated-stage lavas from Niihau, Hawaii, *Geochem. Geophys. Geosyst.*, *9*, Q09005, doi:10.1029/2008GC002076.

Eisele, J., W. Abouchami, S. J. G. Galer, and A. W. Hofmann (2003), The 320 ky Pb isotope evolution of the Mauna Kea lavas recorded in the HSDP-2 drill core, *Geochem. Geophys. Geosyst.*, *4*(5), 8710, doi:10.1029/2002GC000339.

Farnetani, C. G., and A. W. Hofmann (2009), Dynamics and internal structure of a lower mantle plume conduit, *Earth Planet. Sci. Lett.*, *282*, 314–322, doi:10.1016/j.epsl.2009.03.035.

Farnetani, C. G., and A. W. Hofmann (2010), Dynamics and internal structure of the Hawaiian plume, *Earth Planet. Sci. Lett.*, *295*, 231–240, doi:10.1016/j.epsl.2010.04.005.

Farnetani, C. G., A. W. Hofmann, and C. Class (2012), How double volcanic chains sample geochemical anomalies from the lowermost mantle, *Earth Planet. Sci. Lett.*, *359–360*, 240–247, doi:10.1016/j.epsl.2012.09.057.

Fekiacova, Z., W. Abouchami, S. J. G. Galer, M. O. Garcia, and A. W. Hofmann (2007), Origin and temporal evolution of Ko'olau Volcano, Hawaii: Inferences from isotope data on the Ko'olau Scientific Drilling Project (KSDP), the Honolulu volcanics and ODP Site 843, *Earth Planet. Sci. Lett.*, *261*, 65–83, doi:10.1016/j.epsl.2007.06.005.

Frey, F. A., S. Huang, J. Blichert-Toft, M. Regelous, and M. Boyet (2005), Origin of depleted components in basalt related to the Hawaiian hot spot: Evidence from isotopic and incompatible element ratios, *Geochem. Geophys. Geosyst.*, *6*, Q02L07, doi:10.1029/2004GC000757.

Frezzotti, M. L., and A. Peccerillo (2007), Diamond-bearing COHS fluids in the mantle beneath Hawaii, *Earth Planet. Sci. Lett.*, *262*, 273–283, doi:10.1016/j.epsl.2007.08.001.

Galer, S. J. G., and R. K. O'Nions (1985), Residence time of thorium, uranium and lead in the mantle with implications for mantle convection, *Nature*, *316*, 778–782.

Garcia, M. O., and M. Kurz (1991), Reply on "Mahukona: The missing Hawaiian volcano," *Geology*, *19*, 1050–1051.

Garcia, M. O., L. Swinnard, D. Weis, A. R. Greene, T. Tagami, H. Sano, and C. E. Gandy (2010), Petrology, geochemistry and geochronology of Kiaua'i lavas over 4.5 Myr: Implications for the origin of rejuvenated volcanism and the evolution of the Hawaiian plume, *J. Petrol.*, *51*, 1507–1540, doi:10.1093/petrology/egq027.

Gurriet, P. (1987), A thermal model for the origin of post-erosional alkalic lava, Hawaii, *Earth Planet. Sci. Lett.*, *82*, 153–158.

Haase, K. M., M. Regelous, R. A. Duncan, P. A. Brandl, N. Stroncik, and I. Grevemeyer (2011), Insights into mantle composition and mantle melting beneath mid-ocean ridges from postspreading volcanism on the fossil Galapagos rise, *Geochem. Geophys. Geosyst.*, *12*, Q0AC11, doi:10.1029/2010GC003482.

Hanano, D., D. Weis, J. S. Scoates, S. Aciego, and D. J. DePaolo (2010), Horizontal and vertical zoning of heterogeneities in the Hawaiian mantle plume from the geochemistry of consecutive postshield volcano pairs: Kohala-Mahukona and Mauna Kea-Hualalai, *Geochem. Geophys. Geosyst.*, *11*, Q01004, doi:10.1029/2009GC002782.

Hart, S. R. (1984), A large-scale isotope anomaly in the Southern Hemisphere mantle, *Nature*, *309*, 753–757.

Hauri, E. H., J. C. Lassiter, and D. J. DePaolo (1996), Osmium isotope systematics of drilled lavas from Mauna Loa, Hawaii, *J. Geophys. Res.*, *101*, 11,793–11,806.

Hirschmann, M. M., and E. M. Stolper (1996), A possible role for garnet pyroxenite in the origin of the "garnet signature" in MORB, *Contrib. Mineral. Petrol.*, *124*, 185–208.

Hofmann, A. W. (2003), Sampling mantle heterogeneity through oceanic basalts: Isotopes and trace elements, in *Treatise on Geochemistry: The Mantle and Core*, vol. *2*, edited by R. W. Carlson, H. D. Holland, and K. K. Turekian, pp. 61–101, Elsevier, Oxford, U. K.

Hofmann, A. W., and S. R. Hart (1978), An assessment of local and regional isotopic equilibrium in the mantle, *Earth Planet. Sci. Lett.*, *39*, 44–62.

Huang, S., M. Regelous, T. Thordarson, and F. A. Frey (2005), Petrogenesis of lavas from Detroit Seamount: Geochemical differences between Emperor Chain and Hawaiian Volcanoes, *Geochem. Geophys. Geosyst.*, *6*, Q01L06, doi:10.1029/2004GC000756.

Huang, S. C., P. S. Hall, and M. G. Jackson (2011), Geochemical zoning of volcanic chains associated with Pacific hotspots, *Nat. Geosci.*, *4*, 874–878, doi:10.1038/NGEO1263.

Ito, G., and J. J. Mahoney (2005), Flow and melting of a heterogeneous mantle: 2. Implications for a chemically nonlayered mantle, *Earth Planet. Sci. Lett.*, *230*, 47–63.

Katz, R. F., M. Spiegelman, and C. H. Langmuir (2003), A new parameterization of hydrous mantle melting, *Geochim. Geophys. Geosyst.*, *4*(9), 1073, doi:10.1029/2002GC000433.

Kerr, R. A. (2013), The deep Earth machine is coming together, *Science*, *340*, 22–24.

Kerr, R. C., and C. Mériaux (2004), Structure and dynamics of sheared mantle plumes, *Geochem. Geophys. Geosyst.*, *5*, Q12009, doi:10.1029/2004GC000749.

Keshav, S., G. Sen, and D. C. Presnall (2007), Garnet-bearing xenoliths from Salt Lake Crater, Oahu, Hawaii: High-pressure fractional crystallization in the oceanic mantle, *J. Petrol.*, *48*, 1681–1724, doi:10.1093/petrology/egm035.

Kurz, M. D., T. C. Kenna, J. C. Lassiter, and D. J. DePaolo (1996), Helium isotopic evolution of Mauna Kea Volcano: First results from the 1-km drill core, *J. Geophys. Res.*, *101*, 11,781–11,791, doi:10.1029/95JB03345.

O'Neill, H. S. C., and H. Palme (2008), Collisional erosion and the non-chondritic composition of the terrestrial planets, *Philos. Trans. R. Soc. A*, *366*, 4205–4238.

Panning, M., and B. Romanowicz (2006), A three-dimensional radially anisotropic model of shear velocity in the whole mantle, *Geophys. J. Int.*, *167*, 361–379, doi:10.1111/j.1365-246X.2006.03100.x.

Payne, J., M. G. Jackson, and P. S. Hall (2013), Parallel volcano trends and geochemical asymmetry of the Society Islands hotspot, *Geology*, *41*, 19–22, doi:10.1130/G33273.1.

Phipps Morgan, J., and W. J. Morgan (1999), Two-stage melting and the geochemical evolution of the mantle: A recipe for mantle plum-pudding, *Earth Planet. Sci. Lett.*, *170*, 215–239.

Regelous, M., A. W. Hofmann, W. Abouchami, and S. J. G. Galer (2003), Geochemistry of lavas from the Emperor Seamounts, and the geochemical evolution of Hawaiian magmatism from 85 to 42 Ma, *J. Petrol.*, *44*, 113–140.

Ribe, N. M., and U. R. Christensen (1999), The dynamical origin of Hawaiian volcanism, *Earth Planet. Sci. Lett.*, *171*, 517–531, doi:10.1016/S0012-821X(99)00179-X.

Ritsema, J., A. Deuss, H. J. van Heist, and J. H. Woodhouse (2011), S40RTS: A degree-40 shear velocity model for the mantle from new Rayleigh wave dispersion, teleseismic traveltime and normal-mode splitting function measurements, *Geophys. J. Int.*, *184*, 1223–1236.

Romanowicz, B., and Y. Gung (2002), Superplumes from the core-mantle boundary to the lithosphere: Implications for heat flux, *Science*, *296*, 513–516.

Sleep, N. H. (1984), Tapping of magmas from ubiquitous mantle heterogeneities: An alternative to mantle plumes?, *J. Geophys. Res.*, *89*, 10,029–10,041.

Sleep, N. H. (1990), Hotspot and mantle plumes: Some phenomenology, *J. Geophys. Res.*, *95*, 6715–6736.

Sobolev, A. V., et al. (2007), The amount of recycled crust in sources of mantle-derived melts, *Science*, *316*, 412–417.

Spiegelman, M., and P. B. Kelemen (2003), Extreme chemical variability as a consequence of channelized melt transport, *Geochem. Geophys. Geosyst.*, *4*(7), 1055, doi:10.1029/2002GC000336.

Weis, D., M. O. Garcia, J. M. Rhodes, M. Jellinek, and J. S. Scoates (2011), Role of the deep mantle in generating the compositional asymmetry of the Hawaiian mantle plume, *Nat. Geosci.*, *4*, 831–838, doi:10.1038/NGEO1328.

Wirth, R., and A. Rocholl (2003), Nanocrystalline diamond from the Earth's mantle under Hawaii, *Earth Planet. Sci. Lett.*, *211*, 357–369.

Xu, G., F. A. Frey, D. A. Clague, W. Abouchami, J. Blichert-Toft, B. Cousens, and M. Weisler (2007), Geochemical characteristics of West Molokai shield- and postshield-stage lavas: Constraints on Hawaiian plume models, *Geochem. Geophys. Geosyst.*, *8*, Q08G21, doi:10.1029/2006GC001554.

Yaxley, G. M. (2000), Experimental study of the phase and melting relations of homogeneous basalt + peridotite mixtures and implications for the petrogenesis of flood basalts, *Contrib. Mineral. Petrol.*, *139*, 326–338.